ACS chemical biology

Reviews

pubs.acs.org/acschemicalbiology

Sensing Proteins through Nanopores: Fundamental to Applications

Abdelghani Oukhaled,[†] Laurent Bacri,[†] Manuela Pastoriza-Gallego,[†] Jean-Michel Betton,[‡] and Juan Pelta*,[†]

[†]CNRS-UMR 8587, LAMBE, Université de Cergy-Pontoise et Université d'Evry, France

[‡]Unité de Microbiologie Structurale, CNRS-URA 3528, Institut Pasteur, France

ABSTRACT: Proteins subjected to an electric field and forced to pass through a nanopore induce blockades of ionic current that depend on the protein and nanopore characteristics and interactions between them. Recent advances in the analysis of these blockades have highlighted a variety of phenomena that can be used to study protein translocation and protein folding, to probe single-molecule catalytic reactions in order to obtain kinetic and thermodynamic information, and to detect protein−antibody complexes, proteins with DNA and RNA aptamers, and protein−pore interactions. Nanopore design is now well controlled, allowing the development of future biotechnologies and medicine applications.

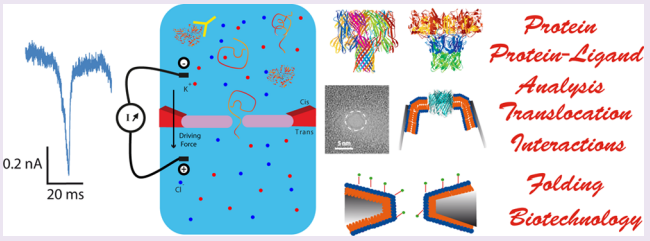

The nanopore, coupled with an electric detection method,[1−6] is a powerful tool to investigate fundamental biological or physical problems at the single-molecule level.[7−9] Some of these issues have been thoroughly studied, such as protein translocation,[10−16] protein folding,[17−20] DNA replication,[21] and enzymatic kinetic reactions.[22−26] Recently strategies have been developed to detect native proteins with aptamers covalently attached to the nanopore.[26−28] Upcoming applications of this method concern biotechnology and medicine,[29] for example, fast sequencing of DNA and RNA,[30,31] bacteria[32] and virus detection,[33,34] single-molecule mass spectrometry,[35,36] and analysis of macromolecular complexes: antibody protein,[37,38] DNA protein.[39] An electrical potential difference is applied to both sides of a lipid or solid-state membrane, separating two isolated chambers, inducing an ionic current through a single pore in the presence of a salt solution. The nanopore is a protein channel or a hole drilled by electron or ion beams.[40,41] Its diameter varies from 2 to 100 nm. A macromolecule passing through this hole induces a decrease in the electrical current by partially blocking the ions, according to the nature of the molecule and the pore characteristics: size, conformation, structure, net charge, geometry, and interactions.[42] The lifetime of an experiment ranges from a few hours, with a lipid bilayer membrane setup, to several hours or a few days, with solid-state membranes.

The study of proteins by single-nanopore recording is a good example of interdisciplinarity: the biology, physics, chemistry, biochemistry, and nanotechnology communities working together. This application of nanopore technology provides a way to probe fundamental biophysical questions and could lead to new biotechnology applications. We review the method to detect protein or protein−ligand complexes using nanopore sensors and how to perform data analysis. We discuss recent results and the great interest for future applications.

One of the main difficulties of the single-nanopore recording technique is to discriminate between the pulses of electric current and the noise and to sort the information from the electrical signal without error due to filter effects. In the first part, we present a detailed efficient data analysis method for protein experiments (Figure 1) and the filter effects on data analysis (Figure 2). The nanopore design and fabrication are crucial for sensing proteins with good sensitivity and also to control dynamics. In the second part, we outline the different nanopores used and the latest strategies to improve these pores (Figure 3), and then we discuss their advantages and limitations. We develop the results and strategies to control protein translocation and interactions (Figure 4) in the third part. The understanding of protein folding remains a challenge. For the past few years, researchers working with nanopores have been exploring this field because this technique allows the observation of individual molecules in different conformations. In the last part, we present studies about protein unfolding and folding (Figure 5) using nanopores. To conclude, we discuss the potential of these applications.

METHOD FOR PROTEIN DATA ANALYSIS AND FILTER EFFECTS

A nanopore connects two compartments filled with an electrolyte solution, separated by a membrane. The application of an electric potential difference *via* two Ag/AgCl electrodes generates an ionic current through the pore. The net charge of a protein is positive or negative according to the pH of the solution. Here, we consider that the driving force is the electric force (Figure 1a). When a protein is driven into the nanopore

Received: August 24, 2012
Accepted: November 10, 2012
Published: November 11, 2012

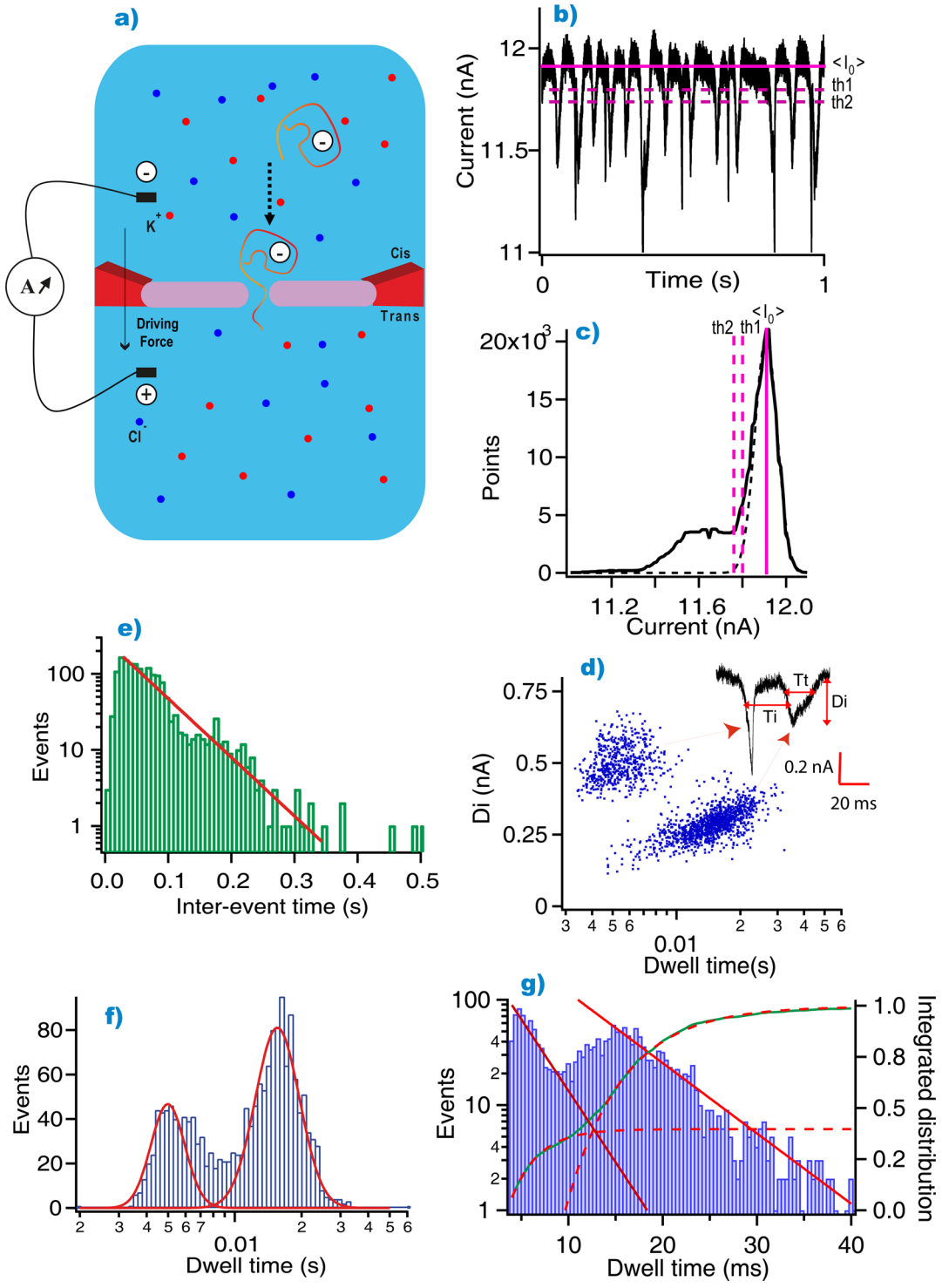

Figure 1. Method for counting individual proteins. (a) Experimental setup. A nanometer hole is drilled into a solid-state membrane, or one channel is inserted into a lipid bilayer, separating two chambers containing electrolytes and where physicochemical conditions are controlled. The membrane is submitted to an electric potential difference that induces an ionic current in the nanopore. The negative electrode of the *cis* side of the compartment, minus sign in the figure, is connected to the ground. We apply the voltage to the electrode of the *trans* side, plus sign in the figure, in order to control the positive potential difference, and then the electrically charged protein (here the protein has a net negative charge) is driven by the applied electrical force toward the *trans* side. (b) Current trace through the nanopore in the presence of unfolded proteins. When a polypeptide chain is transported through the nanopore or interacts with the channel, a decrease in current is observed, because the molecule partially blocks the ions; $\langle I_0 \rangle = 11.90$ nA is the mean open-pore current, $\sigma = 0.05$ nA standard deviation. The first threshold is defined by th1 $= \langle I_0 \rangle - 2\sigma = 11.80$ nA, the second one by th2 $= \langle I_0 \rangle - 3\sigma = 11.75$ nA. (c) Current distribution. We observe two peaks: the first one centered at $\langle I_0 \rangle$ is due to the open-pore current, the second small one is due to the dwelling of proteins. To distinguish the current blockades from the noise, we use both thresholds th1 and th2 (vertical dotted lines). (d) Scatter plot of current variation Di of each event *versus* its dwell time T_t. Three characteristic parameters are defined in the inset: T_i is the inter-event time, and D_i the current variation is due to the dwell of the protein into the nanopore, characterized by the dwell time T_t. (e) Distribution of inter-event intervals T_i. The continuous line is an exponential fit, allowing the calculation of the event frequency $f = 19 \pm 2$ Hz. (f) Logarithmic distribution of the dwell times. The

dx.doi.org/10.1021/cb300449t | *ACS Chem. Biol.* 2012, 7, 1935−1949

Figure 1. continued

curve is a logarithmic normal fit $f(x) = A \exp(-[\ln(x/x_0)]^2/w)$ where A is the amplitude, and x_0 the center and w the width of the distribution; the maximum of the distribution defines the most probable dwell time of 4.9 ± 0.3 ms (short events) and 15.6 ± 1 ms (long ones). (g) (Left axis) Linear distribution of the dwell times, the lines are exponential fits with a characteristic dwell time of 3.2 ± 0.3 ms (short events) and 6.5 ± 0.6 ms (long events). (Right axis) Integrated curve of the dwell time distribution (green color); the red dotted lines are exponential fits with a characteristic dwell time 2.9 ± 0.4 ms (short events) and 5.9 ± 0.5 ms (long events). The experimental conditions are [protein] = 1.56 μM with V = 75 mV, [KCl] = 1 M, at pH = 7.6, pore diameter 20 nm.[15]

and likely through it or interacts with the channel, the recorded current decreases suddenly (Figure 1b). In the case of the Axopatch 200B current amplifier, the cutoff frequency of the internal filter is usually set to f_c = 10 kHz (100 μs). Using the Nyquist−Shannon sampling theorem, the acquisition frequency f_{aq} is at least equal to $2f_c$. Experimentally, it is usually set to f_{aq} = 250 kHz (4 μs). These frequency parameters are usually appropriate for protein translocation or folding experiments. However, we can increase the acquisition frequency (f_{aq} > 1 MHz) according to the capabilities of the acquisition card. In that case, it could be recommended to similarly increase the cutoff frequency of the internal filter of the amplifier. The signal noise is also proportional to the membrane capacitance, which depends mainly on the dielectric constant of the material used in the case of solid-state nanopore and mainly on the hole size on which the lipid bilayer was painted. For instance small holes drilled on conical glass developed by White[43] and used by Reiner[42] provide a more stable and resistance bilayer with a low capacitance. The data processing is based on statistical methods. The baseline corresponds to the noisy ionic current through the empty nanopore defined by its mean value $\langle I_0 \rangle$ (Figure 1b) and its standard deviation (σ). We separate the pulses of electric current from the noise by imposing that a pulse height must be larger than a given threshold in order to be considered as significant. A first threshold th1 is defined by $\langle I_0 \rangle - 2\sigma$ in order to avoid around 95% of the noise fluctuations.[3,42] This threshold, however, is not strong enough; the proteins can approach the pore and just block the current partially. Consequently, it is necessary to apply a higher threshold th2 = $\langle I_0 \rangle - 3\sigma$ in order to distinguish these blockades from the ones due to the dwell events (Figures 1b). This second threshold is checked from the histogram of the electric current of the whole trace. We observe two distinct populations: the first one is associated with the fluctuating baseline current, and the second one corresponds to the blockades (Figure 1c). The width of the pulses T_t is measured at the crossing with the first threshold th1. These spikes are characterized by their frequency ($1/T_i$), duration T_t, and current variation D_i (Figure 1d). From the time position of each event, we plot the distribution of the inter-event time T_i between two consecutive events (Figure 1e). As there is no correlation between events and the interactions between the analyte and the nanopore can be regarded as a reversible chemical reaction,[4] the inter-event distribution corresponds to an exponential described by a Poisson's law. From its exponential fit, we calculate a characteristic inter-event time, which is precisely the inverse of the event frequency f (Figure 1e). The plot of the current variation Di of each spike as a function of its own duration or dwell time T_i is an indication of the protein dynamics into the nanopore: bumping, transport, or interaction events. Interpreting different kinds of blockade signatures caused by RNA interacting with a nanopore was first described by Kasianowicz *et al.*[3] In the case of proteins, in Figure 1d, each scatter is also characterized by a non-specific interaction between a native protein (the maltose binding protein or MBP) and a 20-nm diameter solid-state nanopore. We observe two scatters. The first one, characterized by long durations and low blockades, is explained by the dwelling of one single protein that interacts with the inner side of the nanopore (Figure 1d). This type of event is depicted in the inset of Figure 1d. The second one, with short duration and large blockades, is described by the dwelling of two proteins entering the nanopore in single file: a first protein is entering the pore (a first short gap is observed in the trace of Figure 1d), and just after, it is followed by a second one (second gap in the trace). In this last case, we do not observe interactions between the proteins and the nanopore (short duration), but the current blockade duration is twice that of the first scatter (two proteins are dwelling together). We can study the dwell times more precisely using different distributions and plots. With a logarithmic distribution (Figure 1f) we clearly observe two peaks corresponding to short and long current blockades that characterize both situations described above[15] (Figure 1d). Other Gaussian-like functions could be used, such as the "exponentially modified Gaussian" function.[44] Whatever the function type, the center of the distribution must be located to define the most probable dwell time (Figure 1f). This method is very useful when the amount of data is low, typically around 200 events, as it is usually the case for experiments using solid-state nanopores. However, if the number of events is great enough, around 1000 events, we can plot a linear time distribution (Figure 1g). This representation also allows us to observe both scatters.[15] For duration times other than the most probable times, each time distribution is well fitted by a decreasing exponential function as previously observed with DNA molecules[45,46] and with other polymers.[42,47] From these fits, we calculate the characteristic dwell time of each peak, which could differ from the most probable time. These times correspond to the "temporal dispersion" of dwell times. Sometimes, if the current signal is too noisy or if the number of measured events is too low, we prefer integrating these time distributions in order to decrease the influence of the noise. These integrated distributions (green curve in Figure 1g) are again well fitted by an exponential function, allowing the calculation of the characteristic times. The values of the characteristic times obtained from the time distributions or from the integrated ones have the same magnitude within the error bars. Whatever the chosen time duration (most probable or characteristic time), we note that both time behaviors are the same and that they are proportional.

We now discuss the effects of the filter on data analysis. In the case of small chains, the dwell times are shorter than 100 μs. As the amplifier behaves as a low-pass filter with a cutoff frequency f_c = 10 kHz (T_c = 100 μs) and the acquisition time is 250 kHz (T_{aq} = 4 μs), we can suppose that events shorter than T_c = 100 μs are clearly reduced. In the case of the Axopatch 200B Capacitor Feedback Patch Clamp Amplifier, the filter is a 4-pole Bessel low-pass filter. We have modeled the two types of signal obtained from the data acquisition card. The first one is not reduced by the filter (red trace in Figure 2a,b), and the second one shows the

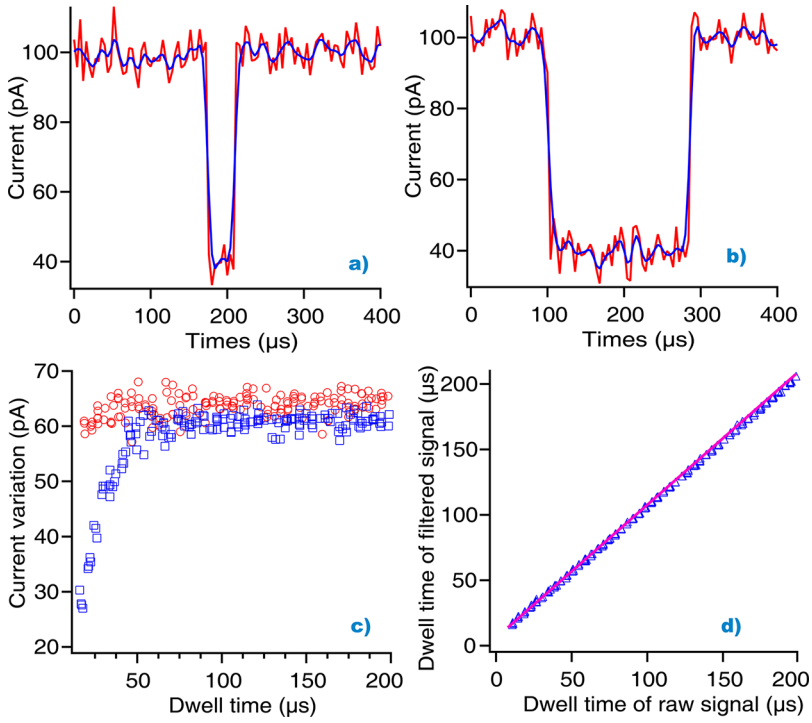

Figure 2. Data analysis and filter effects. Effects of 10 kHz filter on raw data. (a, b) Modeling of the current trace of events. The raw data is in red, and the 10 kHz filtered data is in blue. The modeling of the acquisition time is 4 μs (250 kHz). The events are 38 ± 2 μs long in panel a or 186 ± 2 μs long in panel b. (c) Current variation of each event as a function of its dwell time of raw data (red circles) or filtered data (blue squares). (d) Detected dwell times of filtered signal as a function of the detected dwell time of the raw signal. The straight line is a linear fit $y = a + bx$, where $a = 9 \pm 0.3$ μs and $b = 1.003 \pm 0.002$.

signal reduced by the Bessel filter (blue trace in Figure 2 a,b). If we look at the shape of both traces, we do not observe any difference if the blockade is 38 ± 2 or 136 ± 2 μs long. The high frequency noise is merely smoothed by the filter. Nevertheless, the noise measurements could be relevant. In 1993, it was demonstrated that the spectral density of an open protein channel depends on the ionization of this channel.[48] The first experiments on the transport of neutral polymers through an alamethicin protein channel were conducted using this technique based on noise fluctuation[49] and allowed the first measurements of a chain diffusion coefficient through the channel. The $1/f$ noise measurements were used to separate the maltoporin channel fluctuations from maltose translocation.[50] Recently, these methods were applied to solid-state nanopores (SiN) where the noise reduction, probed by the magnitude of the power spectrum, is a common subject of interest.[51−54] Nevertheless, we observe the same problem for polyethylene terephthalate or glass micropores,[55] nanopores through Al_2O_3 membranes,[56] or single conical nanopores obtained by chemical etching of a single ion-track in polymer film.[57]

In this review, we focus solely on the analysis of individual current blockades. We must take filter effects of the amplifier into account. The method used for the characterization of each event is very important.[58] In our method, the average open pore signal value is I_0 with a standard deviation (σ). All of the current variations larger than 2σ are selected, but we consider only those deeper than 3σ. The duration of each event is calculated from the intersection between the event trace and the $I_0 - 2\sigma$ threshold. This method avoids the rise or fall time effects.[58] The current variation is calculated from the average of the current trace. An example of filter effects is shown in Figure 2c: we consider a computed signal composed of a distribution of blockade durations, increasing continuously from 4 to 200 μs. We plot the measured current variation of each blockade *versus* its duration (dwell time) in both cases. Both plots are similar if the dwell time is larger than 50 μs (Figure 2c). We can note that this time is half the characteristic time of the filter (T_c = 100 μs). Moreover, we can clearly detect the events between 30 and 50 μs, even if they are partially reduced, but this is not the case for the dwell times. We draw the dwell time of the filtered signal *versus* that of the raw signal (Figure 2d): it is linear with a slope equal to 1. From these calculations, we show that the accuracy of the amplifier filter allows only the detection of blockades half the length of its characteristic time T_c. Similar results can be found by another method.[58]

BIOLOGICAL AND BIOMIMETIC NANOPORES

Many proteins need to be transported or translocated across membranes through channels to reach their final location in the cell.[59] Protein translocation usually occurs in an unfolded state and plays an important role in many biological processes: protein import or export toward or from the nucleus, a process that does not require protein unfolding since the nuclear pore is very large (<35 kDa) and protein synthesis and degradation. In general, proteins need to be correctly folded to be functional. Different natural systems of protein transport through lipid membranes are known, but the transport mechanism is still discussed.[60,61] Protein transport through the translocon is associated with protein synthesis, either co-translational or post-translational (Figure 3a). Mimicking these processes artificially at single-molecule level is a challenge. Electrophysiological methods were used to demonstrate the existence of protein-conducting channels.[62,63] Simpler passive channels, generally pore-forming toxins,[64] are used in experiments to explore the field of proteins

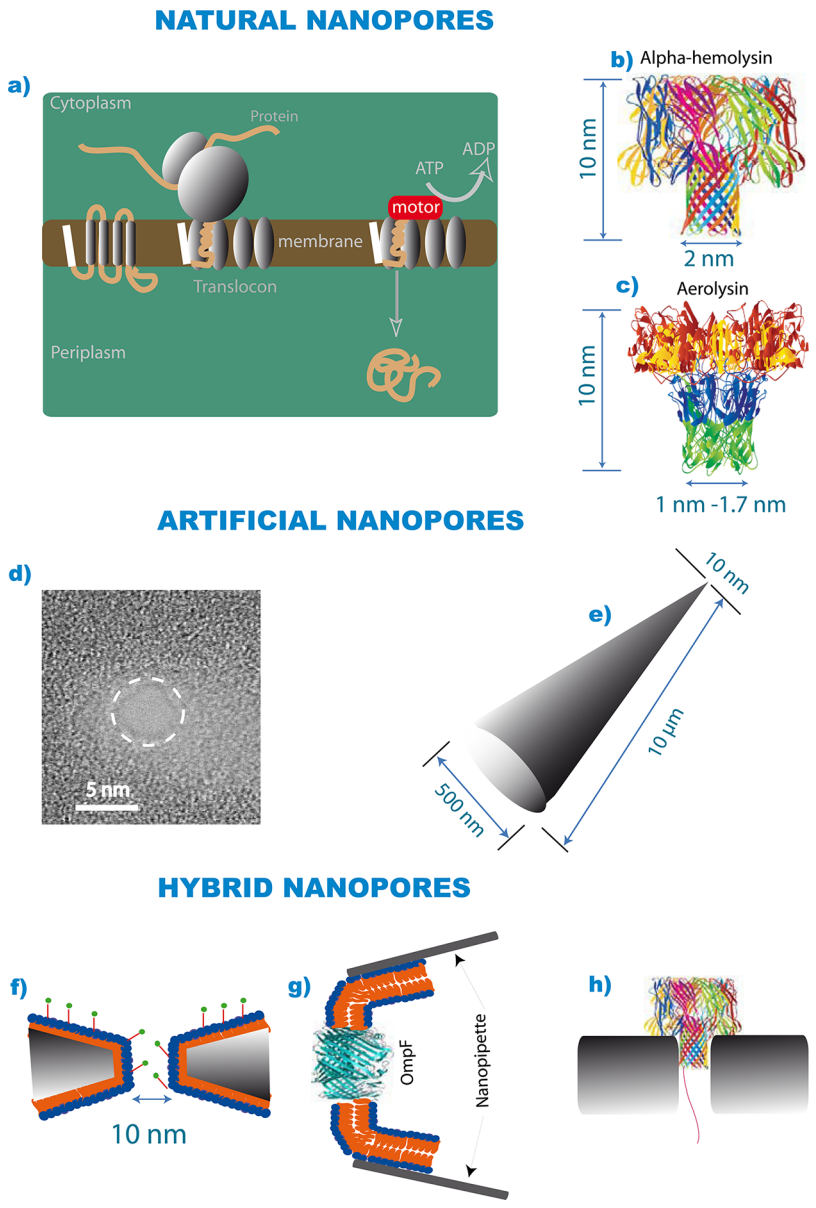

Figure 3. Nanopores used and possibilities for protein sensing. Natural nanopores: (a) Translocation machinery (protein complex) in cells: nascent polypeptides are transported through the membrane of endoplasmic reticulum. Side view of (b) alpha-hemolysin and (c) aerolysin pore; adapted from refs 68 and 73, respectively. These pores are mainly used to study protein translocation, folding, and interactions, because the ionic current of the empty pore is stable. Artificial nanopores: Solid-state nanopores offer the advantage of customized pore diameters and exhibit high mechanical resistance compared that of to natural nanopores inserted in lipid bilayers. d) Image of solid-state nanopore drilled in SiN membrane by an electron beam. (e) Conical nanotube showing its dimensions; adapted from ref 37. Hybrid nanopores: The decoration of solid-state nanopores by direct insertion of natural nanopores or by chemical functionality holds great promise for new applications regarding the sensing of proteins. (f) A solid-state nanopore coated with a fluid lipid bilayer containing ligands attached to the surface that slow down the protein translocation; adapted from ref 14. (g) OmpF porin inserted into a nanopipette containing a lipid bilayer offering high mechanical stability; adapted from ref 89. (h) Alpha-hemolysin channel inserted into a SiN nanopore by attaching a double-strand DNA tail to the channel, which guides the pore into the silicon membrane when voltage is applied; adapted from ref 90.

and nanomedical applications.[29] These experiments consist of inserting a single channel into a model lipid membrane. Most frequently a film of a 1% solution of lipid in decane or other organic solvent is spread across a micrometric wide hole, drilled in a polysulfone or Teflon wall separating the two compartments of a chamber.[65] After thinning of the decane film and formation of a planar bilayer, the channel is inserted by adding a few nanomoles of pore protein. It is also possible to insert a single channel directly by mechanically approaching a hydrogel probe, coated with a layer of protein channels near to a lipid bilayer.[66] The main advantage of the last method is the control of the number of inserted pores, one single pore, without needing to perfuse in order to prevent insertion of other channels. For an overview of fabrication methods of lipid bilayers including supporting membrane, fusion of giant vesicles, and droplet interface bilayers, see ref 67. These membranes are described as a capacitor and a resistor connected in parallel. A great advantage of these lipid bilayers is that we can check their thickness by measuring the capacitance (inversely proportional). We usually observe the insertion of one channel when the membrane is

dx.doi.org/10.1021/cb300449t | *ACS Chem. Biol.* 2012, 7, 1935−1949

thinner than 7 nm. Membranes are stable for several hours. The most used channel is the alpha-hemolysin (Figure 3b) from *Staphylococcus aureus*.[68] This channel is very stable and has been studied in a large range of pH,[69] temperature,[70] salt concentration,[71] and denaturing agents such as urea.[72] Nevertheless, other channels such as aerolysin[73] (Figure 3b) from *Aeromonas hydrophila* or the porin[74] Tom40[75] are also used. The advantage of these biological channels is that their behavior is stable and does not vary throughout the experiment. Their sensitivity is high and their excellent reproducibility is probed by $I-V$ curves. A major advantage of using these channels is that we can make recombinant nanopores by mutagenesis or nanopores modified by covalent and non-covalent chemical modifications.[76] With lipid membranes, the applied voltage is limited to medium voltages (up to 200 mV), since membranes are sensitive to osmotic pressure and chaotropic agents. In general, lipid bilayers break down after 1−10 h of experiment, depending on the solvent used. To bypass this limitation, the biological membranes are replaced by solid-state membranes (Figure 3d); see refs 8 and 77 for some excellent reviews. Different types of membranes can be used, such as silica membranes (Si_3N_4, SiO_2, Al_2O_3), polymer membranes, and recently, graphene membranes.[78] The know-how comes directly from the clean-room of the semiconductor industry. It is possible to obtain solid-state membranes with a thickness between 10 and 50 nm. The nanopore is drilled into the membrane with a diameter between 2 and 100 nm.

For an overview of fabrication techniques and current state of the art methods for nanopore production including sculpting methods, direct drilling, as well as lithographic methods and ion track etching, see ref 79. Two drilling methods are mainly used. The first one uses a gallium focus ion beam (FIB), which hits the surface and drills a nanopore.[40] This FIB is equipped with a feedback mechanism allowing the control of membrane drilling. Alternatively, the ion dose must be calibrated in order to obtain the correct hole size.[80] This technique allows the drilling of both small and large nanopores (3−200 nm). Nevertheless, gallium ions could be inserted into the top few nanometers of the SiN substrate[81] and could charge the inner surface of the nanopore. We can cite another ion source, such as helium, which is focused into a small hole and could allow the fabrication of a nanopore a few nanometers large.[82] This last method promises to produce in one step and in a few minutes large amounts of solid-state nanopores drilled in the same membrane with high production capabilities and the possibility to integrate these fabricated devices into microfluidic devices. The second technique is the most common one: transmission electron microscopy (TEM). A focused electron beam with a spot size less than 10 nm is used to drill a nanopore in a thin membrane. The advantage of the TEM-based technique is the possibility to obtain pores with smaller diameters (up to 1 nm) while watching the pore being drilled.[41] Conical long nanopores are obtained by chemical etching of membrane-based polymers[37,57,83] (Figure 3e). This kind of pore has various specific transport characteristics, exhibiting high current rectification compared to the solid-state nanopore. A recent original system is the nanopipette obtained by pulling standard glass capillaries.[84] The first setup comes from a classical Coulter counter device[85,86] with capillaries of diameters from 2 to 6 μm. By undergoing pulling and heating cycles, the capillaries are thinned and the diameter decreases to 45 nm. The inner side of the nanopipette can be functionalized by several recognition elements.[87] More recently, nanopores are decorated by natural fluids[14,16] (Figure 3f) or by metal deposition[38] in order to control protein translocation and selectivity or by polymer deposition[88] in order to enhance pore selectivity. The solid-state nanopores and nanopipettes allow the use of a hybrid setup (Figure 3g,h).[89,90] An elegant idea has been tested recently: one preassembled protein channel (alpha-hemolysin) attached to DNA is electrophoretically inserted into a narrow hole of a solid-state membrane (Figure 3h). The membrane is very stable for a few days and allows the use of high voltage (up to 900 mV). However, the channel sizes cannot be tailored easily: each nanopore type is characterized by a specific diameter. Electric-field-induced wetting and dewetting in single hydrophobic nanopores due to condensation and evaporation of water in the nanopore has been reported recently.[91]

BACKGROUND TO UNDERSTAND PROTEIN TRANSLOCATION AND PROTEIN−PORE INTERACTIONS

Here we describe how to access some physical parameters relevant in the protein and nanopore field.

Protein-Pore Interactions. If the mean inter-event time (T_i) is linearly dependent on protein concentration (c) and the mean residence time (T_t) is independent of protein concentration, one can assume that the protein partitioning in the pore is governed by a bimolecular interaction between protein and pore. The kinetic rate constant of dissociation (k_{off}) and association (k_{on}) are related to the above measurable characteristic temporal parameters of the binding events T_i and T_t via k_{off} (s^{-1}) = $1/T_t$, and k_{on} (M^{-1} s^{-1}) = $1/(cT_i)$. The dissociation constant is given by K_d (M) = k_{off}/k_{on}, and the association constant is given by K_a (M^{-1}) = $1/K_d$, allowing the calculation of the partitioning coefficient π for the protein between the bulk and the pore, $\pi = K_a c_p$ where c_p (M) is the effective molar concentration of a protein inside the pore. It also allows the calculation of the standard free energy $\Delta G^\circ = -RT \ln K_a$. The free energy of the protein−pore interaction F to overcome the entropic costs of squeezing a protein into a narrow pore can be estimated from the measurable characteristic temporal parameters T_t and the total recording time T_{total}, $F = k_B T \ln(T_t/T_{total})$, where T_t/T_{total} is the measured residence probability (Pr) of the protein within the pore. By measuring the residence probabilities (Pr1), (Pr2) respectively for two proteins of length L1 and L2 within the pore, the variation of the free energy, of entropic origin, is obtained by the relation $F = k_B T \ln(\mathrm{Pr2/Pr1})$. By following the temperature dependence of the association constant at the single molecule level, the standard enthalpy and entropy of the protein-pore interaction can be obtained.

Protein Translocation. If the mean residence time T_t and the mean inter-event time T_i decrease with increasing applied force, T_i decreases with increasing protein concentration, and the residence time increases with increasing peptide length, one can assume that the polypeptide chain is transported through the nanopore. However, if the transport is governed by electrophoresis effects, the mean residence time is expected to be inversely proportional to the applied force. Otherwise, translocating polypeptide chains are traveling in a complex energy landscape with a well-defined energy barrier, and one expects an exponential dependence of the translocation time on the applied force.

If the mean residence time increases linearly as the inverse of the applied voltage increases, the electrophoretic transport theory describes the phenomenon well. Data supporting this concept was provided in ref 3 for single-stranded DNA. The electrophoretic velocity v of protein is related to the electrical field strength by $v = (|z|eE)/(6\pi\eta r)$ where e (C) is the elementary

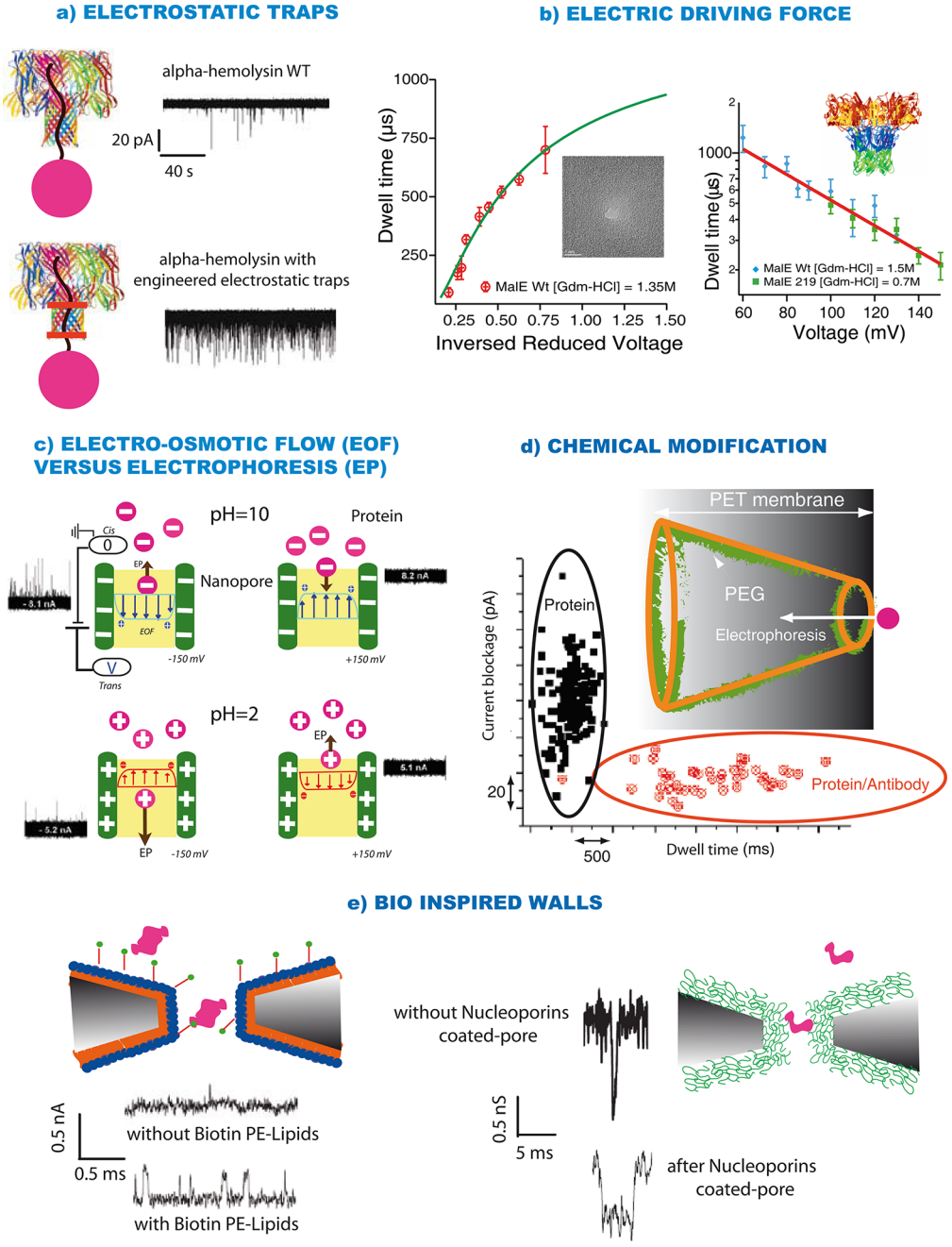

Figure 4. Controlling protein translocation and interactions. (a) Electrostatic traps engineered at the entry and exit of the alpha-hemolysin pore act as binding sites for positively charged proteins and control protein-nanopore interactions; adapted from ref 98. (b) Unfolded proteins transported through a nanopore, controlled by an electrical driving force: (left) with solid-state nanopore; (right) protein channel (aerolysin). The dwell time decreases exponentially with applied electric force at low and medium voltage; adapted from refs 13 and 105. At high voltage the transport time is inversely proportional to the applied voltage.[105] The voltage dependency of the dwell time is well described by the Fokker–Planck model (left). (c) Protein dynamics through solid-state nanopore controlled by electroosmosis flow *versus* electrophoresis; adapted from ref 12. The translocation direction of proteins can be predicted according to the difference in zeta potentials, $\zeta_{protein} - \zeta_{pore}$. At pH = 10 ($|\zeta_{pore}| \gg |\zeta_{protein}|$). Electroosmosis clearly dominates over electrophoresis. At pH = 2 electroosmosis flow weakens the electrophoretic movement, but electrophoresis still dominates. (d) A PEG-functionalized conical gold nanotube can detect and differentiate proteins and protein/antibody complexes because they lead to different current blockade distributions as shown in the scatter plot, adapted from ref 37. (e) Bioinspired synthetic nanopore: (left) with bilayer-coated walls used to slow down translocation of specific proteins after binding to ligands on lipid anchors; adapted from ref 14; (right) with nucleoporins coated-pore in order to make the pore more selective mimicking the nuclear pore complex; adapted from ref 16.

charge, E (V m^{-1}) the electrical field strength proportional to V/L_{pore} (L_{pore} being the pore length), η (Pa s) the viscosity of the solution, and r (m) the radius of the protein. The diffusion coefficient of the protein in solution calculated from the Stokes–Einstein equation is given by $D_{diff} = k_BT/(6\pi\eta r)$. The mean residence time within the pore of length L_{pore} reads as $T_t = \tau = (k_BTL_{pore}^2)/(|z|eD_{diff}V)$ allowing an estimate of the diffusion coefficient of protein in confined geometry. Note that if the transport is purely diffusive the residence time can be estimated by $\tau = L_{pore}^2/D_{diff} = (6\pi\eta r)/(k_BT)L_{pore}^2$.

dx.doi.org/10.1021/cb300449t | *ACS Chem. Biol.* 2012, 7, 1935–1949

If the mean residence time decreases exponentially with the applied force, the chain dynamics are associated with a free-energy barrier. A detailed theory for the effects of the applied potential, which is related directly to the applied force on PEG-induced blockades is provided in ref 42. The data of mean residence time scales as $\tau = a\exp(-V/V_c)$ where a (s), V_c (V) can be extracted from the fit. $V_c = (k_BT)/(z_{inside}e)$ is the critical potential to overcome the entropic costs of squeezing a polypeptide chain into a narrow pore, allowing the estimation of the effective charge z_{inside} of the polypeptide inside the pore.

Generally the frequency data varies exponentially with applied voltage V and is well-described by $f = f_0\exp(|V|/V_0)$ according to the Van't Hoff Arrhenius law $f_0 = (CD_{diff}A/L_{pore})\exp(-U^*/k_BT)$;[92,93] where C (M) and A (m^2) are the polypeptide chain concentration and sectional area of the pore, respectively; f_0 (s^{-1}) is an extrapolated frequency at 0 V and V_0 (V) = $(k_BT)/(ze)$ is the applied potential allowing a charged polypeptide to overcome the Brownian motion; this allows us to estimate the effective charge z at the entrance of the pore. The experimentally obtained value leads to an estimate of the activation energy U^* of entropic and electrostatic origins.

Electro-osmotic (EO) Effects. Electro-osmotic flow (EOF) is a movement of solvent across a charged artificial channel induced by an applied electric potential. The solvent velocity is given by the Smoluchowski equation v_s (m/s) = $(-\varepsilon\varepsilon_0\zeta_{pore}/\eta)E$, where ζ_{pore} (V) is the zeta potential of the channel walls; η is solvent viscosity; ε, ε_0 (F m^{-1}) are the dielectric constant of water and the vacuum permittivity, respectively; and E is the applied electric field. Electro-osmotic flow causes a net solvent flow through the channel that is opposite that of the applied electric field. The electrophoretic (EP) velocity of protein under an external electric field, in the Helmholtz−Smoluchowski limit, is given by v_{prot} (m/s) = $(\varepsilon\varepsilon_0\zeta_{prot}/\eta)E$; the total velocity of protein therefore reads as v (m/s) = $v_{prot} + v_s = (\varepsilon\varepsilon_0E/\eta)(\zeta_{prot} - \zeta_{pore})$.

Pore Conductance and Determining the Size of Proteins with Nanopores. The pore conductance G (S) is the reciprocal of the pore resistance R (Ω), it reads for a cylindrical or conical pore by a series of resistance $R = \rho\int dz/A(z)$, ρ (Ω.m) is the electrolyte resistivity, the z-axis is oriented perpendicular to the membrane surfaces, and $A(z)$ is the cross-sectional area of the pore. Thus, the pore diameter can be estimated from measured current−voltage (I−V) characteristics. The translocation of a protein (assumed to be spherical) through a cylindrical nanopore reduces the current D_i through the pore, directly proportional to the conducting volume excluded by the protein Λ (m^3), which is approximately equal to the volume of the protein, $D_i \approx (E/\rho L_{pore})\Lambda$. The histogram of the current variation D_i is used to estimate the size of the protein. Significant work on this topic for other polymers is reported in refs 42 and 94.

CONTROLLING PROTEIN TRANSLOCATION AND INTERACTIONS

One of the main difficulties of studying protein translocation by a nanopore method is to be sure that the current measurement data, which provide indirect proof, are associated with a true protein transport and not due to non-specific protein binding/unbinding to the protein channel or solid-state nanopore. In the past 10 years, many experiments have been performed with peptides,[10,95,96] proteins,[11,17,19,97,98] or protein−ligand complexes[14,37,38] in order to control the dynamics through the nanopore or specific interactions and also to study enzymatic kinetic reactions.[22−26] These experiments are performed by changing physical parameters, nanopore design and protein structures or net charges[20,99] and by pore surface modification.[37] At the same time, some theoretical work has been performed on biopolymer translocation,[100] peptides, and proteins.[101,102] Models are based on statistical mechanical principles, and biomolecule translocation is described as a diffusion mechanism over energy barriers with two kinds of regime: a capture regime of entropic origin when low force is applied, and a drift regime when high force is applied. Up to now, computer simulations are limited, because biological or experimental time scales of protein transport through channels are several orders of magnitude slower than translocation times accessible to fully atomistic simulations. For example, the transport time of one amino acid through a translocon is estimated at 1−4 ns, and the experimental time is about 1 μs. However, a coarsed-grained approach[103] allows simulations of protein translocation across a nanopore to be performed.[101,102,104]

The first experiment with a passive nanopore (alpha-hemolysin) concerns the structure of peptides investigated by a protein channel.[10] Single, double, or collagen-like triple helical motifs are associated with different spikes, dwell times, and blockade currents. The first study on peptide−pore interaction, with cationic α-helical synthetic peptides and a protein channel (alpha-hemolysin), shows that the association and dissociation rate constants (cf. above paragraph) are strongly dependent on voltage and peptide length. An increase in event frequency has been observed due to an increase in applied voltage and a decrease in event frequency for longer peptides. The different levels of blockade current allow the characterization of these interactions: each level is attributed to a specific chain conformation inside the nanopore, as it was observed with polynucleotides through alpha-hemolysin channel[46] or stretched unfolded proteins through solid state nanopore.[105] Advances in the understanding of protein−pore interactions are due to the development of protein pore engineering.[76] Chemical modification of the β barrel of alpha-hemolysin promotes an electrostatic interaction between the peptide and the pore, reducing the energetic cost of entering the pore (cf. above paragraph), thereby facilitating the translocation of peptides.[106] An elegant study was performed to analyze the mechanism by which a protein containing a single positively charged N-terminal target sequence, similar to the peptide signal sequence necessary for protein transport in the cell, interacts with negatively charged traps engineered within the channel. The electrostatic binding sites at the entry and exit of the pore monitor kinetics of proteins[98] (Figure 4a) and catalyze polypeptide translocation.[107] Furthermore, the engineered pore equipped with aromatic binding sites also facilitates translocation of aromatic peptides and slows down the translocation velocity.[107] An engineered channel was also used to probe enzymatic peptide cleavage.[25] The binding affinity of negatively charged α-helical peptides can also be controlled by the structure and the net charge of the pore.[108]

Other strategies have been developed in order to control the dynamics of proteins through nanopores: protein charge inversion by modulation of the pH,[11,109] controlling the electro-osmotic flow (above paragraph) by modification of both the zeta potential of globular proteins and nanopore,[12] electrical driving force modulation,[13,15,105] chemical surface modifications,[37] and coating nanopore walls with bioinspired fluids.[14,16,38] Recent technical developments allow the investigation of peptide translocation under (MegaHertz) alternating current field.[110] We give some examples of these experiments and

the associated results. Electroosmotic flow regulation by controlling pore walls and protein surface charge allows the modulation of protein dynamics through a solid-state nanopore as a function of pH and positive or negative applied voltage[12] (Figure 4c). Electroosmotic transport enhances or dominates and could reverse electrophoretic transport (Figure 4c). The translocation direction of proteins can be predicted according to the difference between the zeta potentials ($\zeta_{protein} - \zeta_{pore}$); protein diffusion could therefore dominate the transport when the electrophoretic and osmotic forces cancel each other out (above paragraph) (Figure 4c). We can also control the entry and transport of unfolded proteins through protein nanopores with the electric driving force.[13,15] The entry of proteins is described by a Van't Hoff-Arrhenius law associated with an activation barrier (above paragraph). This dependency has been previously observed with DNA,[92] polyelectrolytes[111] with protein channels, and recently with DNA[112] and proteins[15,105] with solid-state nanopores. Recently, it was demonstrated experimentally that the transport of unfolded protein through a narrow solid-state nanopore could be controlled by electric driving force. The protein dwell time decreases exponentially at medium voltage and is inversely proportional at high voltage.[105] This result is consistent with the translocation mechanism where the protein is confined into the pore creating an entropic barrier, followed by electrophoretic transport (Figure 4b). The transport time of unfolded proteins through an aerolysin pore decreases exponentially when the applied voltage increases (Figure 4b), the same dependency was observed with a beta-hairpin peptide through alpha-hemolysin pore.[113] For a double-sized protein, this time is twice that obtained for the single protein at the same voltage.[13] At low voltage, translocating proteins travel in a complex energy landscape with a well-defined energy barrier. At high voltage, the dynamics is dominated by electrophoretical transport (cf. above paragraph).[114] With solid-state nanopores, protein event durations are found many orders of magnitude longer than the electrophoretic transport time.[11,15,19,109,115] This anomalous dynamics is due to the electro-osmotic and protein-pore interaction effects.

Another elegant approach to increase protein or protein–antibody complex captures[116,117] and to reduce the translocation velocity was to coat the pore walls with polymer[37,116] or natural molecules.[14,16,38] The coating is usually created with neutral polymers,[37] and the signature of the protein and complexes is detected by the difference in the dwell time and the blockade current[37] (Figure 4d). Recently, natural lipid bilayers containing anchored mobile ligands have been used to increase temporal and spatial resolution leading to increased protein detection (Figure 4e) and to distinguishing various proteins based on current blockade distribution.[14] The kinetic of beta-amyloid aggregation is also probed by the dynamics of translocation of oligomers and fibril proteins. Nuclear pore proteins are attached to solid-state nanopores (Figure 4e) in order to demonstrate the selective transport of proteins across individual biomimetic nuclear pore complexes. Transport events through the biomimetic nanopore are observed for receptors (Impβ), whereas the passage of non-specific proteins (BSA) is strongly inhibited.[16] Metallized silicon nitride nanopores, chemically modified with receptors, are used to detect subclasses of IgG antibodies.[38] Antibodies are identified according to their specific interaction times with the receptor (protein A). Single nanopore recording was also used to measure protein–DNA interaction with a force spectroscopy setup.[39] This approach allows the determination of association and dissociation rates under equilibrium and non-equilibrium conditions. In particular, it has been used for the measurement of real-time DNA replication.[21] Recently a modified alpha-hemolysin nanopore, by Cu^{2+}-phenanthroline attached covalently to the channel via a cystein, has been used to detect enantiomers of phenylalanine and aspartic amino acids.[118] The current of blockade of each amino acid is different in a mix of these enantiomers.

Chemical modification of the protein channel and genetic engineering has been developed to detect also protein activities and to measure kinetic parameters.[22−26] The alpha-hemolysin channel is chemically modified with a single protein kinase inhibitor peptide attached at the *trans* entrance of the pore. In the presence of the catalytic subunit of cAMP-dependent protein the current traces are altered.[22] From the spikes analysis the kinetic and thermodynamic constants, the peptide–protein interaction are determined. The chemical method is limited because it does not allow to obtain all of the altered subunits in the heteromeric pores modified with one peptide. Genetic engineering was developed to generate heteroheptameric pore containing a single copy of the inhibitor sequence.[23] This elegant approach is powerful tool for the detection of activated kinases and kinase inhibitors. A semisynthetic ion channel or an engineered protein channel were also used to study phosphatase,[24] protease activity,[24] and enzymatic peptide cleavage.[25] In each case the Michaelis constant of the reaction and the rate constant have been determined from current traces analysis. Recently a redesigned stable nanopore fhuA resistant to temperature and acidic pH, in an open state, has been used to probe immunoglobulin G proteolysis by pepsine in acidic buffer solution.[26] During the enzymatic digestion the event frequency of long current blockades decreases, immunoglobulin degradation, as a function of time and the short ones increase, product of digestion, up to the time resolution limit.

PROTEIN FOLDING

The understanding of protein folding remains a great challenge.[119−123] Most experiments to study protein folding *in vitro* are performed in bulk and probe only the average behavior of an ensemble of molecules. However, recent developments in single molecule methods, fluorescence spectroscopy,[124,125] and force spectroscopy AFM[126] and tweezers[127] allow the observation of individual molecules along their folding pathway and give the possibility to explore regions of the energy landscape that are inaccessible to bulk measurements. These techniques provide information on the mechanical stability of proteins, the dynamics, the unfolding intermediates, thermodynamic energy parameters, unfolding rates, and transition state locations.[124−126,128]

Recently, single-nanopore recording has appeared as a new powerful method at single-molecule resolution to study protein folding.[17,129] This technique offers the opportunity to experimentally explore the phase space, to detect rare events, folded proteins with aptamers,[26−28] to separate native, unfolded and partially folded conformations,[15,17,19,20,130] to obtain unfolding curves,[17,20,129] to observe protein mutations,[18,20] to study protein channel stability[70,72] and intrinsically disordered proteins.[18,131]

Since 2007, electrical detection has been used to observe protein denaturation through a single alpha-hemolysin channel as a function of the concentration of chemical denaturing agents, guanidium-HCl[17] (Figure 5a). The ionic current measurements exhibit short and long ionic current blockades (Figure 5b,c). The short blockades are due to the passage of unfolded proteins; their duration remains constant as a function of the concentration of

dx.doi.org/10.1021/cb300449t | *ACS Chem. Biol.* 2012, 7, 1935–1949

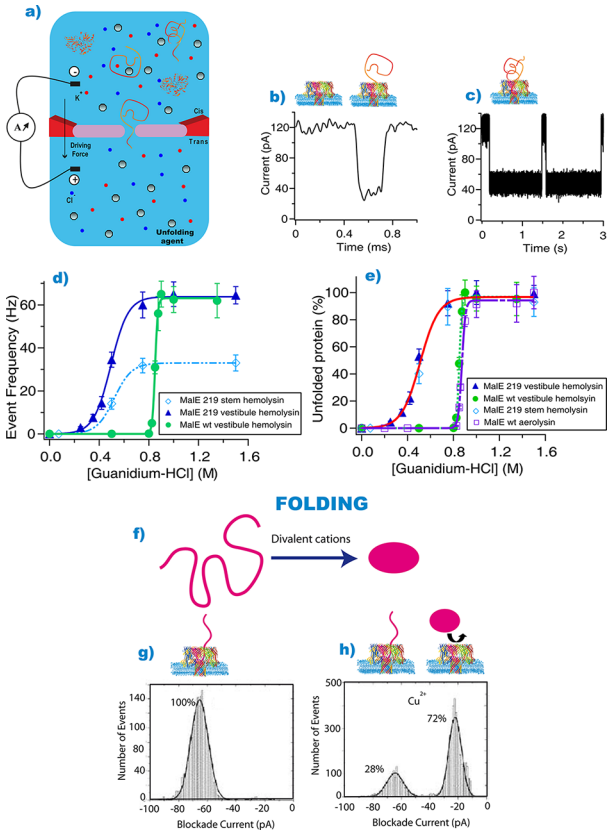

Figure 5. Electrical detection of protein folding. (a) Negatively charged proteins are added to one compartment of the chamber, and the unfolding agent, here guanidium chloride (Guanidium-HCl), a chemical denaturant, is in both compartments at the same concentration. The electric force is the driving force. (b) Detection of unfolded or (c) partially folded protein. (d) Event frequency of current blockades as a function of guanidium chloride concentration. We compare the unfolding of a destabilized variant protein through the vestibule and stem side entry of the alpha-hemolysin pore and the denaturation of the wild type protein (MalEwt). (e) Unfolding curves for wild type protein obtained with an aerolysin pore and an alpha-hemolysin pore and for the destabilized variant; figures adapted from ref 20. (g) Divalent cations induce a compaction of the extended protein. (h) The unfolded or intrinsically disordered protein (myelin basic protein) can translocate the alpha-hemolysin pore. In the presence of divalent cations (Cu^{2+}) the proportion of event translocation (high blockade current) is reduced, and there is a corresponding increase in bumping events (low blockade current); figures adapted from ref 18.

the denaturing agent. Their frequency increases as the concentration of denaturing agent increases following a sigmoidal denaturation curve (Figure 5d). The long blockades are due to the existence of partially folded conformations that block the passage of the proteins (Figure 5c). Their duration decreases as the concentration of denaturing agent increases, and the proteins become more unfolded. This variation of the long blockade as a function of denaturant concentration is adjusted by a Vogel–Tamman–Fulcher law. Models of glass transition, where the variable is the temperature, the distribution of lifetimes is a stretched exponential and the averaged lifetime is given by the Vogel–Tamman–Fulcher law, $t = t_0 \exp[A/(T - T_g)]$. At the transition temperature, the lifetime diverges. This temperature is called the Vogel–Fulcher temperature, T_g. Here, we use a Vogel–Fulcher representation by using as a variable the denaturant concentration (C), guanidium, instead of temperature; $\tau = \tau_0 \exp[A/(C - C_g)]$, τ are the long dwell times of partially folded proteins. These times are the times needed to unfold the protein structures at the pore entrance under the electric driving force. The effect of denaturant on Hydrogen bonds and solvent quality was the same as the one obtained by increasing the temperature. The Vogel–Fulcher law gave the best fit of our data. This is an experimental argument for a possible glassy behavior.[132−134] We try to give a qualitative explanation of the physical effects involved in the dynamic of the partially unfolded protein mechanism rather than a complete theoretical description. In order to evaluate the accuracy of the denaturation transition analysis, an unfolding study of a destabilized protein variant was performed recently, where proteins could enter either by the vestibule or stem side of the pore (Figure 5d). When the proteins enter *via* both sides, the frequency of events follows an identical sigmoidal variation (Figure 5d). But experiments showed a shift of the curves of the destabilized variant toward the lower values of the denaturant agent concentrations compared to the wild type protein. Data normalization showed that the unfolding transition in the denaturation curves does not depend on the pore entry side, geometry, net charge, or structure, applied voltage, or protein concentration (Figure 5e). The unfolding curve obtained with a different nanopore, aerolysin channel, is similar to that obtained with the alpha-hemolysin one.[20] The thermal unfolding transition of a protein has been studied through these two channels. A similar sigmoid normalized event frequency evolution for both nanopores is observed, and the same melting temperature using bulk and single molecule techniques is obtained.[129] Otherwise, it has been observed that the conformation of elastin-like polypeptides attached to alpha-hemolysin pore is sensitive to temperature variations.[135] This paper shows that the current blockades depend on the loop conformation, below the transition temperature the polypeptide is in an expanded conformation and above in a collapse state.

Single solid-state nanopores were also used to study protein unfolding. For the different conformations, folded, partially folded, and unfolded protein (lactoglobulin), the calibrated excluded volumes are estimated from the measure of the amplitude of current blockades, as a function of denaturant concentrations (urea).[19] Data analysis suggests that the measured events are consistent with linear translocation and looped translocation of proteins, even under folded conditions. It was claimed that the nanopore appears to perturb the distribution of protein conformation states in favor of extended conformations. It was shown recently that intrinsically disordered proteins could be studied by a nanopore method[18,131] (Figure 5f). Metal ions induced a folding of small proteins (with zinc finger, myelin basic protein). The transition from disordered to folded protein is probed by the evolution of the ionic current blockades and blockade times according to the nature of the divalent cations and the metal ion concentration. Generally, for disordered molecules, a histogram of current blockades shows one peak centered around 70% of normalized current blockade with long blockade times, probably due to protein transport through the alpha-hemolysin channel (Figure 5g). In the presence of divalent cations, Cu^{2+}, we can observe a decrease in the population of transport events and the appearance of a new peak centered around 20% with short blockade times, associated to a folded protein bumping event. The addition of EDTA, which chelates metal ions, induces the unfolding of the small protein and restores the event profiles to 100% of transport events. It has been shown that the conformation of the prion protein (PrP)

dx.doi.org/10.1021/cb300449t | *ACS Chem. Biol.* 2012, 7, 1935−1949

and prion peptides can be modulated by binding divalent metal ions.[136] Depending on the setup, it is also possible to observe binding events for unfolded protein with protein channels.[72,137] The stability of a pore-forming toxin inside a lipid bilayer as a function of a chemical denaturing agent[72] or temperature[70] was probed. Either the alpha-hemolysin pore is formed before urea denaturation, or the alpha-hemolysin monomer is incubated with urea prior to insertion into a lipid bilayer. For both experimental conditions, the pore remains in the membrane up to high urea concentrations (7.2 M) and channel formation is observed only up to medium denaturant concentrations (4.6 M). A sigmoidal decrease in current amplitude as a function of urea concentration and a loss of current asymmetry are observed, probably associated with vestibule protein denaturation of the channel. Three pores (alpha-hemolysin, Luk and OmpG) were examined as a function of temperature, the channels are formed before temperature increasing. The current increased linearly when the temperature increases up to 93 °C, the changes in single-channel currents are reversible[70]

Recently strategies have been developed to detect native or folded proteins with aptamers attached to the nanopore.[26−28] An oligonucleotide is attached to the pore entrance, vestibule side, of the alpha-hemolysin channel with a disulfide bond. A thrombin aptamer is associated with DNA hybridization to the pore. In the presence of thrombin protein the current level and the frequency of current blockades are altered. Kinetics and thermodynamics parameters determined by the protein−aptamer interaction depend on the aptamer used.[27] Two different DNA aptamers for the binding of thrombin and lysozyme were covalently attached to the *cis* side ClyA nanopore entry. This pore allows the entry of small folded protein inside the channel. In the presence of the aptamers, the selectivity is increased then the frequency of transport events increases for each protein.[28] A robust redesigned nanopore fhuA was used to study the interaction of nucleocapsid viral, NCp7, with different DNA aptamers sequences.[26] Nanopore experiments show that the binding affinity between the nucleocapsid and aptamer depends on the DNA loop sequence.

CONCLUSIONS AND PERSPECTIVES

Nanopores are powerful tools to address fundamental questions about protein dynamics at the single-molecule level and to develop future applications. Each molecule, or complex, is detected by an electric signature *via* the nanopore. Methods to analyze the electric current data are now well established for studying protein translocation, protein unfolding−folding and misfolding, and protein conformation modified by the presence of ligands, to detect both protein-pore interaction and protein−ligand complexes, and to probe enzymatic reaction. However, remaining challenges need to be resolved in order to develop the high potential for biotechnology and medical applications. Up to now, with an electric signal, we have had only indirect proof of the transport of unfolded or native proteins through narrow-diameter nanopores: protein channels, solid-state nanopores, or biomimetic nanopores. We need to prove directly at the nanopore exit the presence of unfolded or folded proteins. We must develop an industrial process to fabricate synthetic nanopores with a perfect control of pore diameters at around 1−2 nm and their hydrophilic properties. It will also be necessary to precisely control the velocity of the protein translocation, without non-specific interactions observed with solid-state nanopores in order to increase the sensitivity. Surface modification with natural fluid is very interesting, as well as chemical functionalization to increase the protein selectivity. Electric and fluorescence signal coupling could be used for protein detection as well used for DNA translocation.[138]

Nanopore sensing could be used to make portable chips at low cost to detect pathologies, misfolded proteins, or antigen−antibody complexes at the single-molecule level. Industrial activity concerning recombinant proteins is an important part of the market of high value-added proteins. However, this production is limited by the incomplete or imperfect folding of the proteins produced. A possible assisted protein refolding through nanopores by perfectly controlling translocation could be used in an industrial process of recombinant protein production. Many pore-forming proteins are involved in human diseases. We can control the formation and the stability of these toxin channels inside a lipid membrane model as a function of the several and different pore environments. This provides a possible future approach to testing antitoxin drugs using nanopore recording techniques in order to prevent toxin formation or to test the level of pathogenicity of a new toxin or variant toxins. Recently, a small viral genome sequencing by nanopore has been performed by the Oxford Nanopore Company. We can plan in the future to develop a setup for the sequencing of peptides and proteins.

AUTHOR INFORMATION

Corresponding Author

*E-mail: Juan.pelta@bio.u-cergy.fr; Jpelta@univ-evry.fr.

Notes

The authors declare no competing financial interest.

ACKNOWLEDGMENTS

This work was supported by grant funding from the Action Thématique Incitative Genopole, and ANR Blanche "TRANS-FOLDPROT" BLAN08-1_339991. We thank K. Foster for kindly correcting the language of the manuscript.

KEYWORDS

Nanopores: natural or artificial holes of nanometer size inside a membrane; **Data acquisition**: data based on the sampling of electric signals, converted into numeric values; **Data analysis**: statistical analysis to discriminate between electric signal and the noise to sort the information from the spikes without error due to filter effects; **Interactions**: term to describe attraction or repulsion between the protein or the complex and the nanopore; **Protein translocation**: transport of proteins through a nanopore; **Protein folding**: the process whereby a protein assumes its three-dimensional and functional shape from a polypeptide chain, unstructured conformation; **Driving force**: the force needed to drive the molecule through the nanopore; **Electrophoresis**: the dynamics of a molecule governed by electric force; **Electro-osmotic flow**: movement of solvent across a charged nanopore induced by an applied electric potential; **Energy barrier**: an energy cost associated with molecule or complex nanopore entry

REFERENCES

(1) Zimmerberg, J., and Parsegian, V. A. (1985) Polymer inaccessible volume changes during opening and closing of a voltage-dependent ionic channel. *Nature 323*, 36−39.

(2) Bezrukov, S. M., Vodyanoy, I., Brutyan, R. A., and Kasianowicz, J. J. (1996) Dynamics and free energy of polymers partitioning into a nanoscale pore. *Macromolecules 29*, 8517−8522.

(3) Kasianowicz, J. J. J., Brandin, E. E., Branton, D. D., and Deamer, D. W. D. (1996) Characterization of individual polynucleotide molecules using a membrane channel. *Proc. Natl. Acad. Sci. U.S.A. 93*, 13770−13773.
(4) Kasianowicz, J. J., and Bezrukov, S. M. (1995) Protonation dynamics of the alpha-toxin ion channel from spectral analysis of pH-dependent current fluctuations. *Biophys. J. 69*, 94−105.
(5) Krasilnikov, O., Sabirov, R., Ternovsky, V., Merzliak, P., and Muratkhodjaev, J. (2005) A simple method for the determination of the pore radius of ion channels in planar lipid bilayer membranes. *FEMS Microbiol. Lett. 105*, 93−100.
(6) Kasianowicz, J. J., Kellermayer, M., Deamer, D. W. (2002) *Structure and Dynamics of Confined Polymers (Nato science 3: Vol. 87) High Technology* (Kasianowicz, J. J., Kellermayer, M., and Deamer, D. W., Eds.) 1st ed., p 408, Springer, New York.
(7) Kasianowicz, J. J., Robertson, J. W. F., Chan, E. R., Reiner, J. E., and Stanford, V. M. (2008) Nanoscopic porous sensors. *Ann. Rev. Anal. Chem. 1*, 737−766.
(8) Howorka, S., and Siwy, Z. (2009) Nanopore analytics: sensing of single molecules. *Chem. Soc. Rev. 38*, 2360.
(9) Movileanu, L. (2009) Interrogating single proteins through nanopores: challenges and opportunities. *Trends Biotechnol. 27*, 333−341.
(10) Sutherland, T. C., Long, Y.-T., Stefureac, R.-I., Bediako-Amoa, I., Kraatz, H.-B., and Lee, J. S. (2004) Structure of peptides investigated by nanopore analysis. *Nano Lett. 4*, 1273−1277.
(11) Fologea, D., Ledden, B., McNabb, D. S., and Li, J. (2007) Electrical characterization of protein molecules by a solid-state nanopore. *Appl. Phys. Lett. 91*, 053901.
(12) Firnkes, M., Pedone, D., Knezevic, J., Döblinger, M., and Rant, U. (2010) Electrically facilitated translocations of proteins through silicon nitride nanopores: conjoint and competitive action of diffusion, electrophoresis, and electroosmosis. *Nano Lett. 10*, 2162−2167.
(13) Pastoriza-Gallego, M., Rabah, L., Gibrat, G., Thiebot, B., van der Goot, F. G., Auvray, L., Betton, J.-M., and Pelta, J. (2011) Dynamics of unfolded protein transport through an aerolysin pore. *J. Am. Chem. Soc. 133*, 2923−2931.
(14) Yusko, E. C., Johnson, J. M., Majd, S., Prangkio, P., Rollings, R. C., Li, J., Yang, J., and Mayer, M. (2011) Controlling protein translocation through nanopores with bio-inspired fluid walls. *Nat. Nanotechnol. 6*, 253−260.
(15) Oukhaled, A., Cressiot, B., Bacri, L., Pastoriza-Gallego, M., Betton, J.-M., Bourhis, E., Jede, R., Gierak, J., Auvray, L., and Pelta, J. (2011) Dynamics of completely unfolded and native proteins through solid-state nanopores as a function of electric driving force. *ACS Nano 5*, 3628−3638.
(16) Kowalczyk, S. W., Kapinos, L., Blosser, T. R., Magalhães, T., van Nies, P., Lim, R. Y. H., and Dekker, C. (2011) Single-molecule transport across an individual biomimetic nuclear pore complex. *Nat. Nanotechnol. 6*, 433−438.
(17) Oukhaled, G., Mathé, J., Biance, A. L., Bacri, L., Betton, J. M., Lairez, D., Pelta, J., and Auvray, L. (2007) Unfolding of proteins and long transient conformations detected by single nanopore recording. *Phys. Rev. Lett.*, 98.
(18) Stefureac, R. I., and Lee, J. S. (2008) Nanopore analysis of the folding of zinc fingers. *Small 4*, 1646−1650.
(19) Talaga, D. S., and Li, J. (2009) Single-molecule protein unfolding in solid state nanopores. *J. Am. Chem. Soc. 131*, 9287−9297.
(20) Merstorf, C., Cressiot, B., Pastoriza-Gallego, M., oukhaled, A., Betton, J.-M., Auvray, L., and Pelta, J. (2012) Wild type, mutant protein unfolding and phase transition detected by single-nanopore recording. *ACS Chem. Biol. 7*, 652−658.
(21) Olasagasti, F., Lieberman, K. R., Benner, S., Cherf, G. M., Dahl, J. M., Deamer, D. W., and Akeson, M. (2010) Replication of individual DNA molecules under electronic control using a protein nanopore. *Nat. Nanotechnol. 5*, 798−806.
(22) Xie, H., Braha, O., Gu, L., Cheley, S., and Bayley, H. (2005) Single-molecule observation of the catalytic subunit of cAMP-dependent protein kinase binding to an inhibitor peptide. *Chem. Biol. 12*, 109−120.
(23) Cheley, S., Xie, H., and Bayley, H. (2006) A genetically encoded pore for the stochastic detection of a protein kinase. *Chem. Eur. J. Chem. Biol. 7*, 1923−1927.
(24) Macrae, M. X., Blake, S., Jiang, X., Capone, R., Estes, D. J., Mayer, M., and Yang, J. (2009) A semi-synthetic ion channel platform for detection of phosphatase and protease activity. *ACS Nano 3*, 3567−3580.
(25) Zhao, Q., de Zoysa, R. S. S., Wang, D., Jayawardhana, D. A., and Guan, X. (2009) Real-time monitoring of peptide cleavage using a nanopore probe. *J. Am. Chem. Soc. 131*, 6324−6325.
(26) Mohammad, M. M. M., Iyer, R. R., Howard, K. R. K., McPike, M. P. M., Borer, P. N. P., and Movileanu, L. L. (2012) Engineering a rigid protein tunnel for biomolecular detection. *J. Am. Chem. Soc. 134*, 9521−9531.
(27) Rotem, D., Jayasinghe, L., Salichou, M., and Bayley, H. (2012) Protein detection by nanopores equipped with aptamers. *J. Am. Chem. Soc. 134*, 2781−2787.
(28) Soskine, M., Biesemans, A., Moeyaert, B., and Cheley, S. (2012) An engineered ClyA nanopore detects folded target proteins by selective external association and pore entry. *Nano Lett. 12*, 4895−4900.
(29) Majd, S., Yusko, E. C., Billeh, Y. N., Macrae, M. X., Yang, J., and Mayer, M. (2010) Applications of biological pores in nanomedicine, sensing, and nanoelectronics. *Curr. Opin. Biotechnol.*, 1−38.
(30) Branton, D., Deamer, D. W., Marziali, A., Bayley, H., Benner, S. A., Butler, T., Di Ventra, M., Garaj, S., Hibbs, A., Huang, X., Jovanovich, S. B., Krstic, P. S., Lindsay, S., Ling, X. S., Mastrangelo, C. H., Meller, A., Oliver, J. S., Pershin, Y. V., Ramsey, J. M., Riehn, R., Soni, G. V., Tabard-Cossa, V., Wanunu, M., Wiggin, M., and Schloss, J. A. (2008) The potential and challenges of nanopore sequencing. *Nat. Biotechnol. 26*, 1146−1153.
(31) Venkatesan, B. M., and Bashir, R. (2011) Nanopore sensors for nucleic acid analysis. *Nat. Nanotechnol. 6*, 615−624.
(32) Guo, P., Hall, E. W., Schirhagl, R., Mukaibo, H., Martin, C. R., and Zare, R. N. (2012) Microfluidic capture and release of bacteria in a conical nanopore array. *Lab Chip 12*, 558−561.
(33) Harms, Z. D., Mogensen, K. B., Nunes, P. S., Zhou, K., Hildenbrand, B. W., Mitra, I., Tan, Z., Zlotnick, A., Kutter, J. P., and Jacobson, S. C. (2011) Nanofluidic devices with two pores in series for resistive-pulse sensing of single virus capsids. *Anal. Chem. 83*, 9573−9578.
(34) Zhou, K., Li, L., Tan, Z., Zlotnick, A., and Jacobson, S. C. (2011) Characterization of hepatitis B virus capsids by resistive-pulse sensing. *J. Am. Chem. Soc. 133*, 1618−1621.
(35) Robertson, J. W. F., Rodrigues, C. G., Stanford, V. M., Rubinson, K. A., Krasilnikov, O. V., and Kasianowicz, J. J. (2007) Single-molecule mass spectrometry in solution using a solitary nanopore. *Proc. Natl. Acad. Sci. U.S.A. 104*, 8207−8211.
(36) Baaken, G., Ankri, N., Schuler, A.-K., Rühe, J., and Behrends, J. C. (2011) Nanopore-based single-molecule mass spectrometry on a lipid membrane microarray. *ACS Nano 5*, 8080−8088.
(37) Sexton, L. T., Horne, L. P., Sherrill, S. A., Bishop, G. W., Baker, L. A., and Martin, C. R. (2007) Resistive-pulse studies of proteins and protein/antibody complexes using a conical nanotube sensor. *J. Am. Chem. Soc. 129*, 13144−13152.
(38) Wei, R., Gatterdam, V., Wieneke, R., Tampé, R., and Rant, U. (2012) Stochastic sensing of proteins with receptor-modified solid-state nanopores. *Nat. Nanotechnol. 7*, 257−263.
(39) Hornblower, B., Coombs, A., Whitaker, R. D., Kolomeisky, A., Picone, S. J., Meller, A., and Akeson, M. (2007) Single-molecule analysis of DNA-protein complexes using nanopores. *Nat. Methods 4*, 315 −317.
(40) Li, J., Stein, D., McMullan, C., Branton, D., Aziz, M. J., and Golovchenko, J. A. (2001) Ion-beam sculpting at nanometre length scales. *Nature 412*, 166−169.
(41) Storm, A. J., Chen, J. H., Ling, X. S., Zandbergen, H. W., and Dekker, C. (2003) Fabrication of solid-state nanopores with single-nanometre precision. *Nat. Mater. 2*, 537−540.

(42) Reiner, J. E., Kasianowicz, J. J., Nablo, B. J., and Robertson, J. W. F. (2010) Theory for polymer analysis using nanopore-based single-molecule mass spectrometry. *Proc. Natl. Acad. Sci. U.S.A. 107*, 12080–12085.
(43) White, R. J. R., Ervin, E. N. E., Yang, T. T., Chen, X. X., Daniel, S. S., Cremer, P. S. P., and White, H. S. H. (2007) Single ion-channel recordings using glass nanopore membranes. *J. Am. Chem. Soc. 129*, 11766–11775.
(44) Langecker, M., Pedone, D., Simmel, F. C., and Rant, U. (2011) Electrophoretic time-of-flight measurements of single DNA molecules with two stacked nanopores. *Nano Lett. 11*, 5002–5007.
(45) Meller, A., Nivon, L., and Brandin, E. (2000) Rapid nanopore discrimination between single polynucleotide molecules. *Proc. Natl. Acad. Sci. U.S.A. 97*, 1079–1084.
(46) Henrickson, S. E., DiMarzio, E. A., Wang, Q., Stanford, V. M., and Kasianowicz, J. J. (2010) Probing single nanometer-scale pores with polymeric molecular rulers. *J. Chem. Phys. 132*, 135101.
(47) Robertson, J. W. F., Rodrigues, C. G., Stanford, V. M., Rubinson, K. A., Krasilnikov, O. V., and Kasianowicz, J. J. (2007) Single-molecule mass spectrometry in solution using a solitary nanopore. *Proc. Natl. Acad. Sci. U.S.A. 104*, 8207–8211.
(48) Bezrukov, S. (1993) Current noise reveals protonation kinetics and number of ionizable sites in an open protein ion channel. *Phys. Rev. Lett. 70*, 2352–2355.
(49) Bezrukov, S. M., Vodyanoy, I., and Parsegian, V. A. (1994) Counting polymers moving through a single ion channel. *Nature 370*, 279–281.
(50) Bezrukov, S. M., and Winterhalter, M. (2000) Examining noise sources at the single-molecule level: 1/f noise of an open maltoporin channel. *Phys. Rev. Lett. 85*, 202–205.
(51) Tabard-Cossa, V., Trivedi, D., Wiggin, M., Jetha, N. N., and Marziali, A. (2007) Noise analysis and reduction in solid-state nanopores. *Nanotechnology 18*, 305505.
(52) Smeets, R. M. M., Keyser, U. F., Dekker, N. H., and Dekker, C. (2008) Noise in solid-state nanopores. *Proc. Natl. Acad. Sci. U.S.A. 105*, 417–421.
(53) Powell, M. R., Sa, N., Davenport, M., Healy, K., Vlassiouk, I., Létant, S. E., Baker, L. A., and Siwy, Z. S. (2011) Noise properties of rectifying nanopores. *J. Phys. Chem. C 115*, 8775–8783.
(54) Rosenstein, J. K., Wanunu, M., Merchant, C. A., Drndić, M., and Shepard, K. L. (2012) Integrated nanopore sensing platform with sub-microsecond temporal resolution. *Nat. Methods 9*, 487–492.
(55) Uram, J. D., Ke, K., and Mayer, M. (2008) Noise and bandwidth of current recordings from submicrometer pores and nanopores. *ACS Nano 2*, 857–872.
(56) Venkatesan, B. M., Dorvel, B., Yemenicioglu, S., Watkins, N., Petrov, I., and Bashir, R. (2009) Highly sensitive, mechanically stable nanopore sensors for DNA analysis. *Adv. Mater. 21*, 2771–2776.
(57) Siwy, Z., and Fuliński, A. (2002) Fabrication of a Synthetic Nanopore Ion Pump. *Phys. Rev. Lett. 89*, No. 198103.
(58) Pedone, D., Firnkes, M., and Rant, U. (2009) Data analysis of translocation events in nanopore experiments. *Anal. Chem. 81*, 9689–9694.
(59) Schatz, G., and Dobberstein, B. (1996) Common principles of protein translocation across membranes. *Science 271*, 1519–1526.
(60) Wickner, W. (2005) Protein translocation across biological membranes. *Science 310*, 1452–1456.
(61) Rapoport, T. A. (2007) Protein translocation across the eukaryotic endoplasmic reticulum and bacterial plasma membranes. *Nature 450*, 663–669.
(62) Simon, S. M., and Blobel, G. (1991) A protein-conducting channel in the endoplasmic reticulum. *Cell 65*, 371–380.
(63) Fèvre, F., Henry, J. P., and Thieffry, M. (1994) Reversible and irreversible effects of basic peptides on the mitochondrial cationic channel. *Biophys. J. 66*, 1887–1894.
(64) Iacovache, I., van der Goot, F. G., and Pernot, L. (2008) Pore formation: An ancient yet complex form of attack. *Biochim. Biophys. Acta, Biomembr. 1778*, 1611–1623.
(65) Meuller, P., Rudin, D. O., Tien, H. T., and Wescott, W. C. (1962) Reconstitution of cell membrane structure in vitro and its transformation into an excitable system. *Nature 194*, 979–980.
(66) Holden, M. A., and Bayley, H. (2005) Direct introduction of single protein channels and pores into lipid bilayers. *J. Am. Chem. Soc. 127*, 6502–6503.
(67) Bayley, H., Cronin, B., Heron, A., Holden, M. A., Hwang, W. L., Syeda, R., Thompson, J., and Wallace, M. (2008) Droplet interface bilayers. *Mol. BioSyst. 4*, 1191–1208.
(68) Song, L., Hobaugh, M. R., Shustak, C., Cheley, S., Bayley, H., and Gouaux, J. E. (1996) Structure of staphylococcal alpha-hemolysin, a heptameric transmembrane pore. *Science 274*, 1859–1866.
(69) Bezrukov, S. M., and Kasianowicz, J. J. (1997) The charge state of an ion channel controls neutral polymer entry into its pore. *Eur. Biophys. J. 26*, 471–476.
(70) Kang, X.-F., Gu, L.-Q., Cheley, S., and Bayley, H. (2005) Single protein pores containing molecular adapters at high temperatures. *Angew. Chem., Int. Ed. 44*, 1495–1499.
(71) Oukhaled, G., Bacri, L., Mathé, J., Peelta, J., and Auvray, L. (2008) Effect of screening on the transport of polyelectrolytes through nanopores. *EPL 82*, 48003.
(72) Pastoriza-Gallego, M., Oukhaled, G., Mathé, J., Thiebot, B., Betton, J.-M., Auvray, L. C., and Pelta, J. (2007) Urea denaturation of α-hemolysin pore inserted in planar lipid bilayer detected by single nanopore recording: Loss of structural asymmetry. *FEBS Lett. 581*, 3371–3376.
(73) Parker, M. W., Buckley, J. T., Postma, J. P., Tucker, A. D., Leonard, K., Pattus, F., and Tsernoglou, D. (1994) Structure of the Aeromonas toxin proaerolysin in its water-soluble and membrane-channel states. *Nature 367*, 292–295.
(74) Baslé, A., Rummel, G., Storici, P., Rosenbusch, J. P., and Schirmer, T. (2006) Crystal structure of osmoporin OmpC from E. coli at 2.0 Å. *J. Mol. Biol. 362*, 933–942.
(75) Mahendran, K. R., Romero-Ruiz, M., Schlösinger, A., Winterhalter, M., and Nussberger, S. (2012) Protein translocation through Tom40: kinetics of peptide release. *Biophys. J. 102*, 39–47.
(76) Bayley, H., and Jayasinghe, L. (2004) Functional engineered channels and pores (Review). *Mol. Membr. Biol. 21*, 209–220.
(77) Dekker, C. (2007) Solid-state nanopores. *Nat. Nanotechnol. 2*, 209–215.
(78) Garaj, S., Hubbard, W., Reina, A., Kong, J., Branton, D., and Golovchenko, J. A. (2010) Graphene as a subnanometre trans-electrode membrane. *Nature*, 1–5.
(79) Healy, K., Schiedt, B., and Morrison, A. P. (2007) Solid-state nanopore technologies for nanopore-based DNA analysis. *Nanomedicine 2*, 875–897.
(80) Schiedt, B., Auvray, L., Bacri, L., Oukhaled, G., Madouri, A., Bourhis, E., Patriarche, G., Pelta, J., Jede, R., and Gierak, J. (2010) Direct FIB fabrication and integration of "single nanopore devices" for the manipulation of macromolecules. *Microelectron. Eng. 87*, 1300–1303.
(81) Unocic, K. A., Mills, M. J., and Daehn, G. S. (2010) Effect of gallium focused ion beam milling on preparation of aluminium thin foils. *J. Microsc. 240*, 227–238.
(82) Yang, J., Ferranti, D. C., Stern, L. A., Sanford, C. A., Huang, J., Ren, Z., Qin, L.-C., and Hall, A. R. (2011) Rapid and precise scanning helium ion microscope milling of solid-state nanopores for biomolecule detection. *Nanotechnology 22*, 285310.
(83) Mara, A., Siwy, Z., Trautmann, C., Wan, J., and Kamme, F. (2004) An asymmetric polymer nanopore for single molecule detection. *Nano Lett. 4*, 497–501.
(84) Umehara, S., Pourmand, N., Webb, C. D., Davis, R. W., Yasuda, K., and Karhanek, M. (2006) Current rectification with poly-L-lysine-coated quartz nanopipettes. *Nano Lett. 6*, 2486–2492.
(85) Coulter, W. Patent US2656508, 1956.
(86) Neher, E., Sakmann, B., and Steinbach, J. H. (1978) The extracellular patch clamp: a method for resolving currents through individual open channels in biological membranes. *Pflugers Arch. 375*, 219–228.

(87) Umehara, S., Karhanek, M., Davis, R. W., and Pourmand, N. (2009) Label-free biosensing with functionalized nanopipette probes. *Proc. Natl. Acad. Sci. U.S.A. 106*, 4611−4616.
(88) Ali, M., Yameen, B., Cervera, J., Ramírez, P., Neumann, R., Ensinger, W., Knoll, W., and Azzaroni, O. (2010) Layer-by-layer assembly of polyelectrolytes into ionic current rectifying solid-state nanopores: insights from theory and experiment. *J. Am. Chem. Soc. 132*, 8338−8348.
(89) Gornall, J. L., Mahendran, K. R., Pambos, O. J., Steinbock, L. J., Otto, O., Chimerel, C., Winterhalter, M., and Keyser, U. F. (2011) Simple reconstitution of protein pores in nano lipid bilayers. *Nano Lett. 11*, 3334−3340.
(90) Hall, A. R., Scott, A., Rotem, D., Mehta, K. K., Bayley, H., and Dekker, C. (2010) Hybrid pore formation by directed insertion of α-haemolysin into solid-state nanopores. *Nat. Nanotechnol. 5*, 874−877.
(91) Powell, M. R., Cleary, L., Davenport, M., Shea, K. J., and Siwy, Z. S. (2011) Electric-field-induced wetting and dewetting in single hydrophobic nanopores. *Nat. Nanotechnol. 6*, 798−802.
(92) Henrickson, S. E., Misakian, M., Robertson, B., and Kasianowicz, J. J. (2000) Driven DNA transport into an asymmetric nanometer-scale pore. *Phys. Rev. Lett. 85*, 3057−3060.
(93) Ambjörnsson, T., Apell, S. P., Konkoli, Z., Di Marzio, E. A., and Kasianowicz, J. J. (2002) Charged polymer membrane translocation. *J. Chem. Phys. 117*, 4063.
(94) Krasilnikov, O., Rodrigues, C., and Bezrukov, S. (2006) Single polymer molecules in a protein nanopore in the limit of a strong polymer-pore attraction. *Phys. Rev. Lett. 97*, No. 018301.
(95) Sanchez-Quesada, J., Ghadiri, M. R., Bayley, H., and Braha, O. (2000) Cyclic peptides as molecular adapters for a pore-forming protein. *J. Am. Chem. Soc. 122*, 11757−11766.
(96) Movileanu, L., Schmittschmitt, J. P., Martin Scholtz, J., and Bayley, H. (2005) Interactions of peptides with a protein pore. *Biophys. J. 89*, 1030−1045.
(97) Stefureac, R., Waldner, L., Howard, P., and Lee, J. S. (2008) Nanopore analysis of a small 86-residue protein. *Small 4*, 59−63.
(98) Mohammad, Prakash, S., Matouschek, A., and Movileanu, L. (2008) Controlling a single protein in a nanopore through electrostatic traps. *J. Am. Chem. Soc. 130*, 4081−4088.
(99) Christensen, C., Baran, C., Krasniqi, B., Stefureac, R. I., Nokhrin, S., and Lee, J. S. (2011) Effect of charge, topology and orientation of the electric field on the interaction of peptides with the α-hemolysin pore. *J. Peptide Sci. 17*, 726−734.
(100) Muthukumar, M. (2001) Translocation of a confined polymer through a hole. *Phys. Rev. Lett. 86*, 3188−3191.
(101) Makarov, D. E. (2009) Computer simulations and theory of protein translocation. *Acc. Chem. Res. 42*, 281−289.
(102) Bacci, M., Chinappi, M., Casciola, C. M., and Cecconi, F. (2012) Role of denaturation in maltose binding protein translocation dynamics. *J. Phys. Chem. B 116*, 4255−4262.
(103) Hyeon, C., and Thirumalai, D. (2011) Capturing the essence of folding and functions of biomolecules using coarse-grained models. *Nat. Commun. 2*, 487−487.
(104) Chinappi, M., Cecconi, F., and Casciola, C. M. (2011) Computational analysis of maltose binding protein translocation. *Philos. Mag. 91*, 2034−2048.
(105) Cressiot, B., oukhaled, A., Patriarche, G., Pastoriza-Gallego, M., Betton, J.-M., Auvray, L., Muthukumar, M., Bacri, L., and Pelta, J. (2012) Protein transport through a narrow solid-state nanopore at high voltage: experiments and theory. *ACS Nano 6*, 6236−6243.
(106) Wolfe, A. J., Mohammad, C., S., Bayley, H., and Movileanu, L. (2007) Catalyzing the translocation of polypeptides through attractive interactions. *J. Am. Chem. Soc. 129*, 14034−14041.
(107) Wolfe, A. J., Mohammad, C., S., Bayley, H., and Movileanu, L. (2007) Catalyzing the translocation of polypeptides through attractive interactions. *J. Am. Chem. Soc. 129*, 14034−14041.
(108) Stefureac, R., Long, Y.-T., Kraatz, H.-B., Howard, P., and Lee, J. S. (2006) Transport of α-helical peptides through α-hemolysin and aerolysin pores. *Biochemistry 45*, 9172−9179.
(109) Han, A., Creus, M., Schürmann, G., Linder, V., Ward, T. R., de Rooij, N. F., and Staufer, U. (2008) Label-free detection of single protein molecules and protein−protein interactions using synthetic nanopores. *Anal. Chem. 80*, 4651−4658.
(110) Stefureac, R. I., Kachayev, A., and Lee, J. S. (2012) Modulation of the translocation of peptides through nanopores by the application of an AC electric field. *Chem. Commun. 48*, 1928.
(111) Brun, L., Pastoriza-Gallego, M., Oukhaled, G., Mathé, J., Bacri, L., Auvray, L., and Pelta, J. (2008) Dynamics of polyelectrolyte transport through a protein channel as a function of applied voltage. *Phys. Rev. Lett.*, 100.
(112) Kowalczyk, S. W., Tuijtel, M. W., Donkers, S. P., and Dekker, C. (2010) Unraveling single-stranded DNA in a solid-state nanopore. *Nano Lett. 10*, 1414−1420.
(113) Goodrich, C. P., Kirmizialtin, S., Huyghues-Despointes, B. M., Zhu, A., Scholtz, J. M., Makarov, D. E., and Movileanu, L. (2007) Single-molecule electrophoresis of β-hairpin peptides by electrical recordings and Langevin dynamics simulations. *J. Phys. Chem. B 111*, 3332−3335.
(114) Muthukumar, M. (2009) *Polymer Translocation*, p 354, CRC, Boca Raton.
(115) Niedzwiecki, D. J., Grazul, J., and Movileanu, L. (2010) Single-molecule observation of protein adsorption onto an inorganic surface. *J. Am. Chem. Soc. 132*, 10816−10822.
(116) Siwy, Z. Z., Trofin, L. L., Kohli, P. P., Baker, L. A. L., Trautmann, C. C., and Martin, C. R. C. (2005) Protein biosensors based on biofunctionalized conical gold nanotubes. *J. Am. Chem. Soc. 127*, 5000−5001.
(117) Uram, J. D., Ke, K., Hunt, A. J., and Mayer, M. (2006) Label-free affinity assays by rapid detection of immune complexes in submicrometer pores. *Angew. Chem., Int. Ed. Engl. 45*, 2281−2285.
(118) Boersma, A. J. A., and Bayley, H. H. (2012) Continuous stochastic detection of amino Acid enantiomers with a protein nanopore. *Angew. Chem., Int. Ed. Engl. 51*, 9606−9609.
(119) Onuchic, J. N., Luthey-Schulten, Z., and Wolynes, P. G. (1997) Theory of protein folding: the energy landscape perspective. *Annu. Rev. Phys. Chem. 48*, 545−600.
(120) Dobson, C. M. (2003) Protein folding and misfolding. *Nature 426*, 884−890.
(121) Dill, K., Ozkan, S., and Shell, M. (2008) The protein folding problem. *Annu. Rev. Biophys. 37*, 289−316.
(122) Bartlett, A. I., and Radford, S. E. (2009) An expanding arsenal of experimental methods yields an explosion of insights into protein folding mechanisms. *Nat. Struct. Mol. Biol. 16*, 582−588.
(123) Freddolino, P., Harrison, C., and Liu, Y. (2010) Challenges in protein-folding simulations. *Nat. Phys. 6*, 751−758.
(124) Michalet, X. X., Weiss, S. S., and Jäger, M. M. (2006) Single-molecule fluorescence studies of protein folding and conformational dynamics. *Chem. Rev. 106*, 1785−1813.
(125) Schuler, B., and Eaton, W. A. (2008) Protein folding studied by single-molecule FRET. *Curr. Opin. Struct. Biol. 18*, 16−26.
(126) Fisher, T. E., Marszalek, P. E., and Fernandez, J. M. (2000) Stretching single molecules into novel conformations using the atomic force microscope. *Nat. Struct. Biol. 7*, 719−724.
(127) Moffitt, J., Chemla, Y., and Smith, S. (2008) Recent advances in optical tweezers. *Annu. Rev. Biochem. 77*, 205−228.
(128) Borgia, A., Williams, P. M., and Clarke, J. (2008) Single-molecule studies of protein folding. *Biochemistry 77*, 101−125.
(129) Payet, L. L., Martinho, M. M., Pastoriza-Gallego, M. M., Betton, J.-M. J., Auvray, L. L., Pelta, J. J., and Mathé, J. J. (2012) Thermal unfolding of proteins probed at the single molecule level using nanopores. *Anal. Chem. 84*, 4071−4076.
(130) Freedman, K. J., Jürgens, M., Prabhu, A., Ahn, C. W., Jemth, P., Edel, J. B., and Kim, M. J. (2011) Chemical, thermal, and electric field induced unfolding of single protein molecules studied using nanopores. *Anal. Chem. 83*, 5137−5144.
(131) Baran, C., Smith, G. S. T., Bamm, V. V., Harauz, G., and Lee, J. S. (2010) Divalent cations induce a compaction of intrinsically disordered myelin basic protein. *Biochem. Biophys. Res. Commun. 391*, 224−229.

(132) Iben, I., Braunstein, D., Doster, W., Frauenfelder, H., Hong, M., Johnson, J., Luck, S., Ormos, P., Schulte, A., Steinbach, P., Xie, A., and Young, R. (1989) Glassy behavior of a protein. *Phys. Rev. Lett. 62*, 1916−1919.
(133) Frauenfelder, H., Sligar, S. G., and Wolynes, P. G. (1991) The energy landscapes and motions of proteins. *Science 254*, 1598−1603.
(134) Brujić, J., Hermans, R, Walther, K. M., and Fernandez, J. M. (2006) Single-molecule force spectroscopy reveals signatures of glassy dynamics in the energy landscape of ubiquitin. *Nat. Phys. 2*, 282−286.
(135) Jung, Y., Bayley, H., and Movileanu, L. (2006) Temperature-responsive protein pores. *J. Am. Chem. Soc. 128*, 15332−15340.
(136) Stefureac, R. I., Madampage, C. A., Andrievskaia, O., and Lee, J. S. (2010) Nanopore analysis of the interaction of metal ions with prion proteins and peptides. *Biochem. Cell Biol. 88*, 347−358.
(137) Pastoriza-Gallego, M., Gibrat, G., Thiebot, B., Betton, J.-M., and Pelta, J. (2009) Polyelectrolyte and unfolded protein pore entrance depends on the pore geometry. *Biochim. Biophys. Acta, Biomembr. 1788*, 1377−1386.
(138) Heron, A. J., Thompson, J. R., Cronin, B., Bayley, H., and Wallace, M. I. (2009) Simultaneous measurement of ionic current and fluorescence from single protein pores. *J. Am. Chem. Soc. 131*, 1652−1653.